25th ABCM International Congress of Mechanical Engineering
October 20-25, 2019, Uberlândia, MG, Brazil

COB-2019-0711
THREE-DIMENSIONAL IDENTIFICATION OF A HUMANOID ROBOT

Caroline Cristine Duarte da Silva
Daniela Vacarini de Faria
Davi Herculano Vasconcelos Barroso
Marcos Ricardo Omena de Albuquerque Maximo
Luiz Carlos Sandoval Góes
Instituto Tecnológico de Aeronáutica (ITA)-Praça Marechal Eduardo Gomes, 50 - Vila das Acácias, 12228-900- São José dos Campos - SP/Brasil
carolcds@ita.br
danivacarini@gmail.com
herculanodavi@gmail.com
mmaximo@ita.br
goes@ita.br

Abstract. *This work proposes the identification of parameters of a humanoid research robot, in particular Robotis DARwIn OP2. The methodology followed is based on a consolidated identification technique combined with the Statically Equivalent Serial Chains (SESC) method, the input data chosen for the system are the angles of the robotic joints. Initially, this methodology was tested on a simulator, produced by the Laboratório de Sistemas Computacionais Autonômos (LAB-SCA) of ITA. Later this methodology was be applied in a real robot, Robotis DARwIn OP2, also available at LAB-SCA.*

Keywords: *Humanoid Robotics, System Identification, Kinematic Chain*

1. INTRODUCTION

Bipedal walking, a key factor to creating functional humanoid robots, is a complex field of knowledge from the point of view of control, due to non linearity, underactuation and high number of degrees of freedom, representing a great challenge to the latest generation control techniques (Collins *et al.*, 2005). What makes humanoid robotics so fascinating is the similarity with humans, enabling interaction with human tools and human environments.

A widely accepted approach for bipedal walking, the 3D Linear Inverted Pendulum Model (3D-LIPM) (Kajita *et al.*, 2001), allows one to obtain the CoM trajectory and then, by inverse kinematics, determine the joint angles during the walk. Because of the simplifications of the model, we often use strategies of feedback and compensation of dynamic error to improve the robot's stability (Takenaka *et al.*, 2009). Therefore, the parameters of the robotic system need to be well defined.

In order to guarantee the stability of bipedal walking robots, it is important to ensured that the point where the sum of reaction forces are null (known as Center of Pressure, or CoP) lies within a polygon of defined as the convex envelope of the contact points between the robot and the ground (Vukobratović and Borovac, 2004). In static cases, the CoP coincides with the projection of center of mass (CoM) on the ground.

Based on this, it is intended to use different values of the CoP, at each position that the robot performs. The parameter identification method suggested in this paper consists in using a set of postures to find the combination of mass and center of mass of the body parts of the robot. The equation that describes the three-dimensional kinematic chain is obtained through the SESC method.

In the Literature, there are works of parameter estimation using ground contact force, in (Cotton *et al.*, 2009) a HOAP3 humanoid robot has its parameters two-dimensionally identified using the sensors at one of its feet. In (van Zutven, 2014) the humanoid robot TUlip has its parameters three-dimensionally identified using a force platform. In this work, we propose a three-dimensional identification using sensors on the feet of a humanoid research robot, Robotis OP2 shown in Fig. 1a.

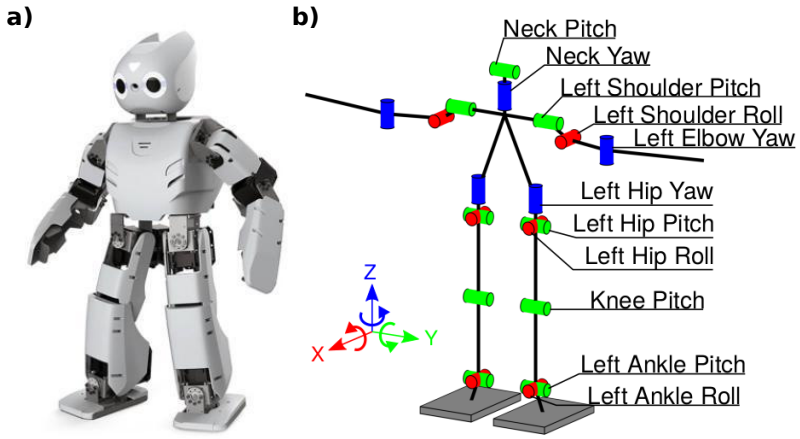

Figure 1. a) Robotis OP2 humanoid robot. b) A schematic drawing that shows the robot's degrees of freedom, the names of the right-side joints are similar to the left-side ones shown here.

2. METHODOLOGY

2.1 Least Square Method

For the identification, the least squares estimator is used , since it is capable of determining unknown parameters of a mathematical model capable of adjusting optimally to the noisy observations of the input and output of the system. Following the final equation of the procedure done by (Coelho and Coelho, 2004), it relates Y (measured vector of CoP) to the parameter vector estimate ($\hat{\mathbf{\Theta}}$) through a regression matrix ($\mathbf{\Phi}$) that is a function of the inputs in the system.

$$\hat{\mathbf{\Theta}} = [\mathbf{\Phi}^T \mathbf{\Phi}]^{-1} \mathbf{\Phi}^T \mathbf{Y}. \tag{1}$$

2.2 SESC method

In a given posture, a kinematic chain is formed by n links and each link has a joint of revolution. Each link is fully described by its geometric and mass properties. The SESC method allows finding the resulting center of mass of the chain. Homogeneous transformations, denoted $\mathbf{T}_i \in \mathbb{R}^{4\times4}$, are used to relate the local reference points of the system (Cotton *et al.*, 2009):

$$\mathbf{T}_i = \begin{bmatrix} \mathbf{A}_i & \mathbf{d}_i \\ \mathbf{0} & 1 \end{bmatrix} \tag{2}$$

where $\mathbf{A}_i \in \mathbb{R}^{3\times3}$ is a rotation matrix, $\mathbf{d}_i \in \mathbb{R}^3$ is the displacement vector between the local reference points and $\mathbf{0} \in \mathbb{R}^3$.

The DoF of Robotis OP2 are distributed in the following manner: 2 in the neck, 3 in each arm and 6 in each leg, Fig. 1 b. Each DoF of this humanoid robot is implemented by a servomotor. In Fig. 1 b, the servomotor denoted by the blue color performs only rotation around Z, the green color only rotation around Y, the red color only rotation around X. We considered the global reference point at the center of the right foot sole in Eq. (3).

To set which parts have the parameters that will be combined, generally we have the vector $\mathbf{c}_i \in \mathbb{R}^3$ used to locate the CoM of a body relative to a local reference and masses (m_i) of the 21 body parts, Fig. 2.

In Tab. 1 is contained the relationship between the parts of of the robot and the index i of the parameters shown in Fig. 2.

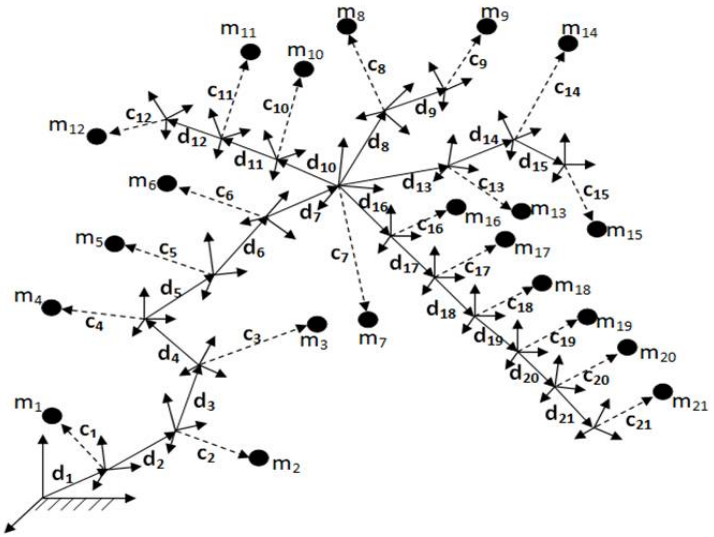

Figure 2. A drawing of the kinematic chain.

Table 1. Relation between the parts of the robot and the index i.

Index	Body Part	Index	Body Part
1	right foot	12	right arm
2	right ankle	13	left shoulder
3	right tibia	14	left elbow
4	right thigh	15	left arm
5	right pelvis	16	left hip
6	right hip	17	left pelvis
7	torso	18	left thigh
8	neck	19	left tibia
9	head	20	left ankle
10	right shoulder	21	left foot
11	right elbow		

$$
\begin{aligned}
\begin{bmatrix}\mathbf{CoM}\\ 1\end{bmatrix} \;=\; & \frac{m_1\mathbf{T}_1\begin{bmatrix}\mathbf{c}_1\\1\end{bmatrix}}{M}+\frac{m_2\mathbf{T}_{1:2}\begin{bmatrix}\mathbf{c}_2\\1\end{bmatrix}}{M}+\frac{m_3\mathbf{T}_{1:3}\begin{bmatrix}\mathbf{c}_3\\1\end{bmatrix}}{M}+\frac{m_4\mathbf{T}_{1:4}\begin{bmatrix}\mathbf{c}_4\\1\end{bmatrix}}{M}+\frac{m_5\mathbf{T}_{1:5}\begin{bmatrix}\mathbf{c}_5\\1\end{bmatrix}}{M}+\frac{m_6\mathbf{T}_{1:6}\begin{bmatrix}\mathbf{c}_6\\1\end{bmatrix}}{M}\\
& +\frac{m_7\mathbf{T}_{1:7}\begin{bmatrix}\mathbf{c}_7\\1\end{bmatrix}}{M}+\frac{m_8\mathbf{T}_{1:8}\begin{bmatrix}\mathbf{c}_8\\1\end{bmatrix}}{M}+\frac{m_9\mathbf{T}_{1:9}\begin{bmatrix}\mathbf{c}_9\\1\end{bmatrix}}{M}+\frac{m_{10}\mathbf{T}_{1:7}\mathbf{T}_{10}\begin{bmatrix}\mathbf{c}_{10}\\1\end{bmatrix}}{M}+\frac{m_{11}\mathbf{T}_{1:7}\mathbf{T}_{10:11}\begin{bmatrix}\mathbf{c}_{11}\\1\end{bmatrix}}{M}\\
& +\frac{m_{12}\mathbf{T}_{1:7}\mathbf{T}_{10:12}\begin{bmatrix}\mathbf{c}_{12}\\1\end{bmatrix}}{M}+\frac{m_{13}\mathbf{T}_{1:7}\mathbf{T}_{13}\begin{bmatrix}\mathbf{c}_{13}\\1\end{bmatrix}}{M}+\frac{m_{14}\mathbf{T}_{1:7}\mathbf{T}_{13:14}\begin{bmatrix}\mathbf{c}_{14}\\1\end{bmatrix}}{M}+\frac{m_{15}\mathbf{T}_{1:7}\mathbf{T}_{13:15}\begin{bmatrix}\mathbf{c}_{15}\\1\end{bmatrix}}{M}\\
& +\frac{m_{16}\mathbf{T}_{1:7}\mathbf{T}_{16}\begin{bmatrix}\mathbf{c}_{16}\\1\end{bmatrix}}{M}+\frac{m_{17}\mathbf{T}_{1:7}\mathbf{T}_{16:17}\begin{bmatrix}\mathbf{c}_{17}\\1\end{bmatrix}}{M}+\frac{m_{18}\mathbf{T}_{1:7}\mathbf{T}_{16:18}\begin{bmatrix}\mathbf{c}_{18}\\1\end{bmatrix}}{M}+\frac{m_{19}\mathbf{T}_{1:7}\mathbf{T}_{16:19}\begin{bmatrix}\mathbf{c}_{19}\\1\end{bmatrix}}{M}\\
& +\frac{m_{20}\mathbf{T}_{1:7}\mathbf{T}_{16:20}\begin{bmatrix}\mathbf{c}_{20}\\1\end{bmatrix}}{M}+\frac{m_{21}\mathbf{T}_{1:7}\mathbf{T}_{16:21}\begin{bmatrix}\mathbf{c}_{21}\\1\end{bmatrix}}{M}
\end{aligned}
\tag{3}
$$

where $\mathbf{T}_{i:j} = \mathbf{T}_i\mathbf{T}_{i+1}\ldots\mathbf{T}_{j-1}\mathbf{T}_j$.

By placing the rotational matrices, the following equation is obtained, where the vector $\mathbf{r}_i \in \mathbb{R}^3$ represents the parameter combinations.

$$\begin{aligned}\mathbf{CoM} &= \mathbf{d}_1 + \mathbf{B}_1\mathbf{r}_1 + \mathbf{B}_2\mathbf{r}_2 + \mathbf{B}_3\mathbf{r}_3 + \mathbf{B}_4\mathbf{r}_4 + \mathbf{B}_5\mathbf{r}_5 + \mathbf{B}_6\mathbf{r}_6 + \mathbf{B}_7\mathbf{r}_7 + \mathbf{B}_8\mathbf{r}_8 + \mathbf{B}_9\mathbf{r}_9 + \mathbf{B}_{10}\mathbf{r}_{10} \\ &+\mathbf{B}_{11}\mathbf{r}_{11} + \mathbf{B}_{12}\mathbf{r}_{12} + \mathbf{B}_{13}\mathbf{r}_{13} + \mathbf{B}_{14}\mathbf{r}_{14} + \mathbf{B}_{15}\mathbf{r}_{15} + \mathbf{B}_{16}\mathbf{r}_{16} + \mathbf{B}_{17}\mathbf{r}_{17} + \mathbf{B}_{18}\mathbf{r}_{18} \\ &+\mathbf{B}_{19}\mathbf{r}_{19} + \mathbf{B}_{20}\mathbf{r}_{20} + \mathbf{B}_{21}\mathbf{r}_{21} \end{aligned} \tag{4}$$

with $\mathbf{B}_1 = \mathbf{A}_1$, $\mathbf{B}_2 = \mathbf{A}_1\mathbf{A}_2$, $\mathbf{B}_3 = \mathbf{B}_2\mathbf{A}_3$, $\mathbf{B}_4 = \mathbf{B}_3\mathbf{A}_4$, $\mathbf{B}_5 = \mathbf{B}_4\mathbf{A}_5$, $\mathbf{B}_6 = \mathbf{B}_5\mathbf{A}_6$, $\mathbf{B}_7 = \mathbf{B}_6\mathbf{A}_7$, $\mathbf{B}_8 = \mathbf{B}_7\mathbf{A}_8$, $\mathbf{B}_9 = \mathbf{B}_8\mathbf{A}_9$, $\mathbf{B}_{10} = \mathbf{B}_7\mathbf{A}_{10}$. $\mathbf{B}_{11} = \mathbf{B}_{10}\mathbf{A}_{11}$, $\mathbf{B}_{12} = \mathbf{B}_{11}\mathbf{A}_{12}$,$\mathbf{B}_{13} = \mathbf{B}_7\mathbf{A}_{13}$, $\mathbf{B}_{14} = \mathbf{B}_{13}\mathbf{A}_{14}$. $\mathbf{B}_{15} = \mathbf{B}_{14}\mathbf{A}_{15}$, $\mathbf{B}_{16} = \mathbf{B}_7\mathbf{A}_{16}$, $\mathbf{B}_{17} = \mathbf{B}_{16}\mathbf{A}_{17}$, $\mathbf{B}_{18} = \mathbf{B}_{17}\mathbf{A}_{18}$, $\mathbf{B}_{19} = \mathbf{B}_{18}\mathbf{A}_{19}$. $\mathbf{B}_{20} = \mathbf{B}_{19}\mathbf{A}_{20}$, $\mathbf{B}_{21} = \mathbf{B}_{20}\mathbf{A}_{21}$.

In this case, only the right foot of the Robotis OP2 will be in contact all the time on the ground. Each position of the robot in "XYZ" has a projection point of CoM in "XY", this point is the $CoP = (CoM_x, CoM_y)$. Finally, there is the estimator in Eq. (5), where '-p' indicates pseudo-inverse, $\mathbf{B}_i \in \mathbb{R}^{2\times3}$ and n indicates the number of measurements taken.

In fact what can be determined is a combination of the parameters, the great reason being the lack of observability of the parameters separately. The vector $\mathbf{r_i}$, found in Eq. (5), contains the combination of these parameters, which in our scenario is an arrangement of CoM and masses. The maximum number of positions can be infinite, but the minimum number of positions must be equal to the number of $\mathbf{r_i}$.

$$\begin{bmatrix}\mathbf{r}_1\\ \vdots \\ \mathbf{r}_{21}\end{bmatrix} = \left[\begin{bmatrix}\mathbf{B}_1 & \dots & \mathbf{B}_{21}\\ \vdots & \vdots & \vdots \\ \mathbf{B}_n & \vdots & \vdots\end{bmatrix}_{2n\times66}\right]^{-p} \begin{bmatrix}CoM_{x1}\\ CoM_{y1}\\ \vdots \\ CoM_{xn}\\ CoM_{yn}\end{bmatrix}_{2n} \tag{5}$$

3. SIMULATION RESULTS

At first, a simulator based on Maximo (2017) was used, since this simulator uses manufacturer data. As system inputs, randomly sampled joint angles with uniform distribution were used, ranging from -30 to 30 degrees. In order to make the collection of CoPs more realistic, Gaussian noise of null mean and standard deviation of 0.00493 was added to the measurements. These parameters were based on real foot sensor data (Ha *et al.*, 2013). A data set of 1000 different positions was used. The results were than compared to data from the manufacturer, as shown in Fig. 3a, where R_i is the magnitude of the vector $\mathbf{r}_i$.

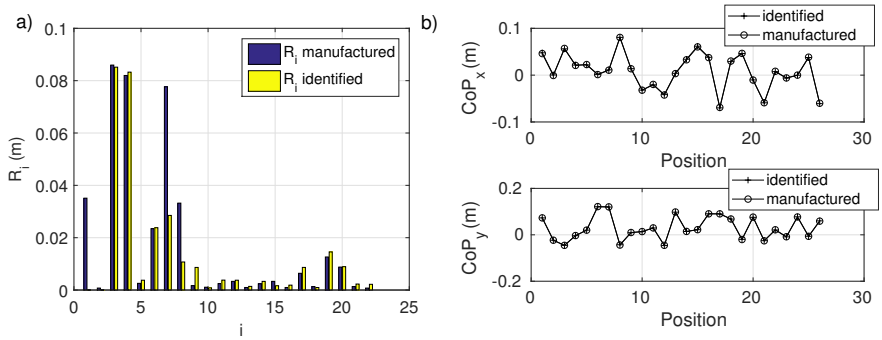

Figure 3. a) Comparison between R_i manufactured and identified .b) Comparison of CoP_x and CoP_y.

It was noted that both simulated R_1 and R_2 were not identified, for R_1 this occurs because $\mathbf{c}_1$ is equal to $\mathbf{d}_1$. And for R_2 this occurs because $\mathbf{A}_2$ is an identity matrix, therefore it has no observability. The R_i values are clearly not exactly the same, the reason for this is the lack of observability in consecutive revolutions on the same axis. Then, to analyze the R_i we will compare the values of the CoPs, since this is enough to multiply the $\mathbf{r}_i$, referring to each R_i, by the matrix in Eq. (5), whose dimension $\in \mathbb{R}^{2n\times66}$. In Fig. 3b, it is shown that both CoP_x and CoP_y are identical for R_i manufactured and identified, for image resolution purposes 26 positions are taken from the 1000 positions.

In practice, for control purposes we are only interested in the position of the CoP. So individual values of R_i's are not important, as long as the estimated CoP values match the simulated CoP values. Therefore the identification is satisfactory for the Robotis OP2, with an mean absolute error between the estimate CoPs and the measured CoPs of 0.0040 for $n = 1000$.

4. EXPERIMENT

The second part of the analysis consisted on applying the same chain obtained by the SECS on the real robot. Utilizing the gravity compensation (Maximo, 2017), to ensure that the robot's joints remain in the desired places. Positions were obtained that allowed the robot to have static stability, and using a sensor located at the foot of Robotis OP2, we collected the CoP values.

Since the robot should be in a standing position, only stable poses could be used. To obtain these poses, angular constraints were imposed to the joints, because without these restrictions there could be loss of stability or shocks between the parts of the robot. Figure 4 illustrates how the servos are arranged in Robotis OP2. The robot pose shown in the figure is how the robot initializes its movements, i.e, in this position the angles of all the servos are zero.

Figure 4 shows the IDs of each servo (Robotis OP2, 2019), in the Tab. 2 shows the minimum and maximum angles of each servo. In our convention, negative values represent clockwise rotations and positive values represent counter-clockwise rotations. For to maintain the stability, a restriction was also placed on the CoP, which must be restricted to a location inside the polygon determined by the foot sensors, then we choose the CoP following constraint values for: $-0.023m < CoP_x < 0.023m$ and $-0.023m < CoP_y < 0.023m$.

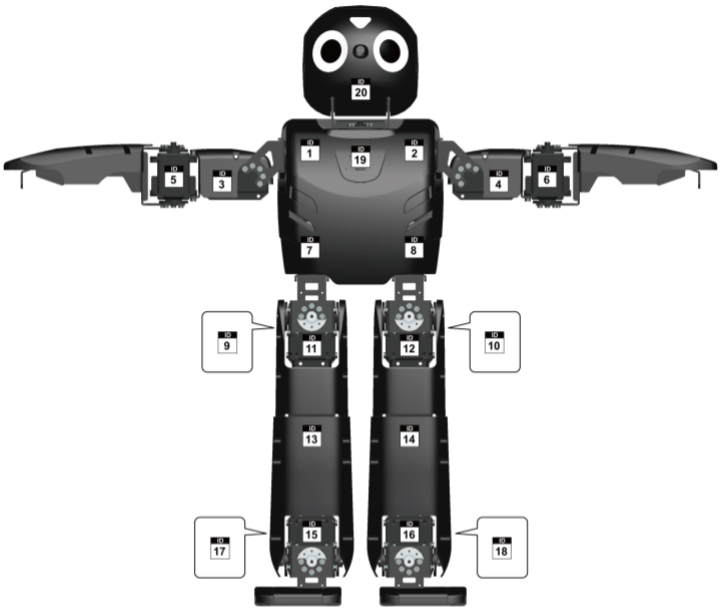

Figure 4. Starting position,(Robotis OP2, 2019).

After this, the experiment was performed, Fig. 5 shows some poses of the experiment. All poses were measured by the sensor ROBOTIS OP2-FSR (force sensing resistor), located on the right foot of the robot. In total, 38 valid poses were obtained. Since the sensor is very noisy, each CoP measurement was obtained from the mean value of 100 sensor readings for each pose.

4.1 Experimental Results

Figure 6 illustrates the comparison between the R_i predicted using the data provided by the manufacturer and the ones identified by the experiment. The result shows that R_i values differ, although Fig. 6 is not enough to build a comparison, since similarly to simulation we have lack of observability. Then, to analyze R_i, we compared the values of the measured and estimated CoPs.

In Fig. 7 the comparison between the CoPs is illustrated. In Fig. 7a the black curve represents the theoretical CoP_x – the value of CoP_x found with the R_i found with the data povided by the manufacturer – the red curve represents the CoP_x measured in the experiment and the blue curve represents the CoP_x obtained using the R_i found in the experiment. Note that the CoP_x found using the manufacturer's data follows a similar trend to the measured CoP_x, but has a clear offset. Nevertheless, the identified values of CoP_x are close to the experimental ones. The small differences probably come from model imperfection. Indeed, we observed that Robotis OP2 joints have substantial backlash, thus there is considerable uncertainty on joints positions.

In Fig. 7b, the black curve represents the theoretical CoP_y, the red curve represents the CoP_y measured in the experiment and the curve blue represents the CoP_y using the R_i found in the experiment. CoP_y's behavior is very similar to

Table 2. Range of the angles.

ID	Minimum Angulation (degree)	Maximum Angulation (degree)
1	$-180°$	$180°$
2	$-180°$	$180°$
3	$-120°$	$84°$
4	$-84°$	$120°$
5	$-4°$	$156°$
6	$-156°$	$4°$
7	$-50°$	$30°$
8	$-30°$	$50°$
9	$-57°$	$5°$
10	$-5°$	$57°$
11	$-29°$	$96°$
12	$-29°$	$96°$
13	$0°$	$132°$
14	$0°$	$132°$
15	$-79°$	$51°$
16	$-79°$	$51°$
17	$-57°$	$37°$
18	$-37°$	$57°$
19	$-120°$	$120°$
20	$-40°$	$25°$

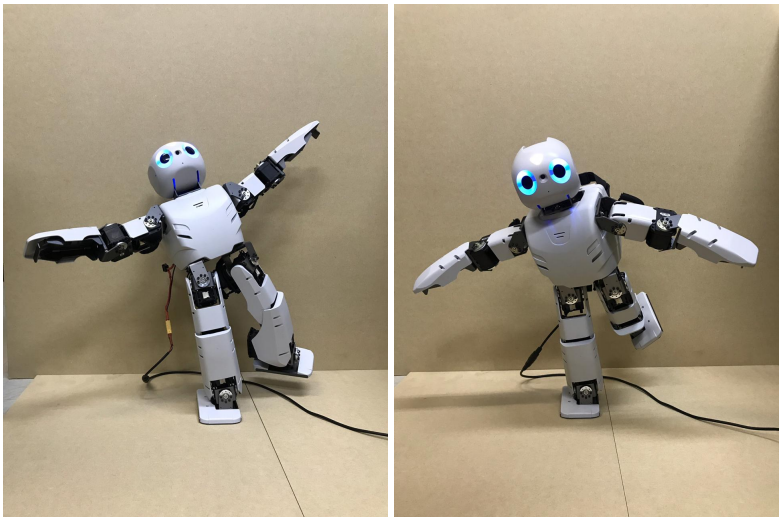

Figure 5. Example of balance pose for the experiment.

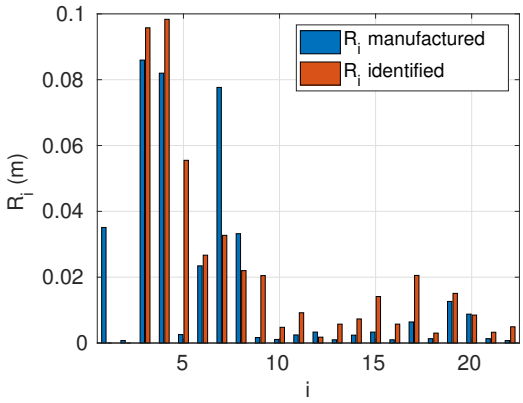

Figure 6. Comparison between R_i predicted and identified.

CoP_x's behavior.

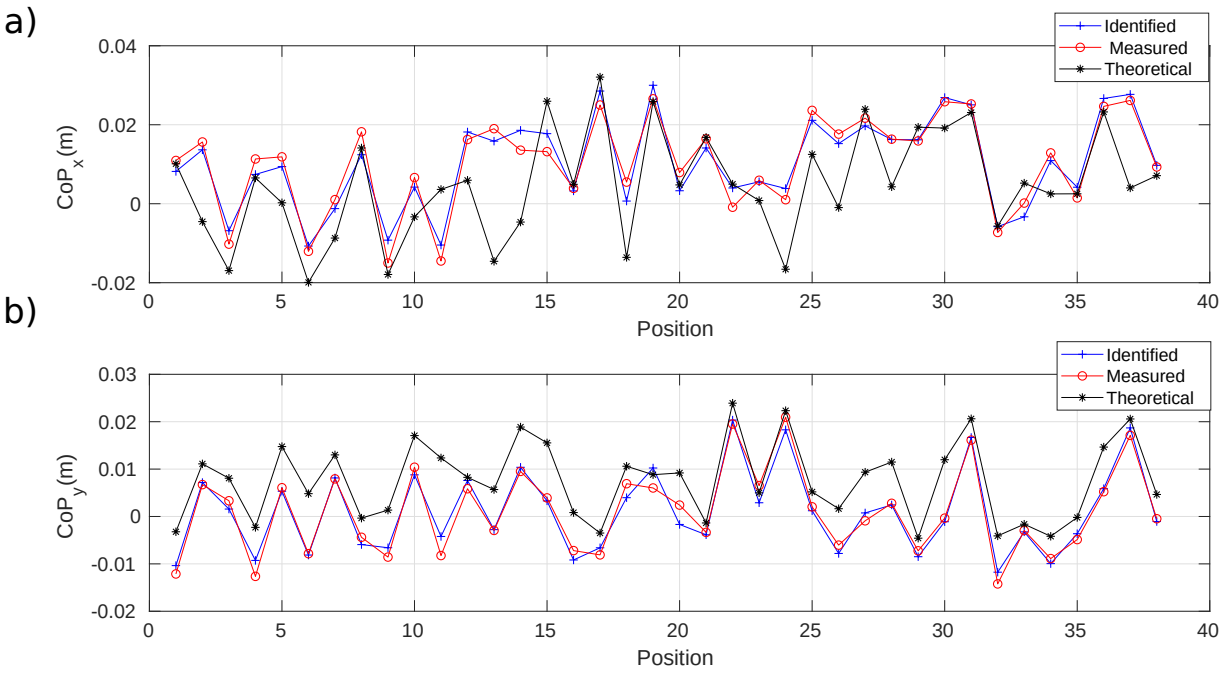

Figure 7. Comparison between CoPs.

Another interesting result that can be obtained using this technique is to find the height of the CoM, meaning that flat measurements of the CoP can be used to find a third component of the CoM: the CoM_z. It is important to emphasize that the CoM_z has a huge impact on walking dynamics.

In Fig. 8, the blue curve represents the values of CoM_z from the R_i identified in the experiment and black curve represents the values of CoM_z for the R_i obtained with data from the manufacturer. In fact, the values do not coincide, which was already expected since the CoPs (shown in Fig. 7) presented an offset.

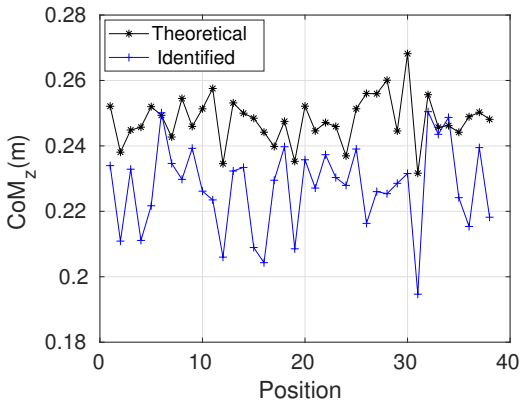

Figure 8. CoM height.

5. CONCLUSION

The technique used in this paper proved quite useful, since for a walking model of the humanoid robot it is necessary to use the combinations of parameters, in the case of the article indicated by R_i. We hypothesize that the difference between the values found between the experiment and the manufacturer's data is due to the fact that the manufacturer uses data from CAD drawings and does not take into account components such as screws, wires and electronic boards.

The great importance of the identification experiment is that, in fact, we are now able to obtain values closer to the real values of the parameters, which is of paramount importance for the dynamic models. Therefore, in the future we intend to use the data obtained by identification for a refinement of the dynamic model used in our walking algorithm, expecting that this could render a more stable walk.

6. ACKNOWLEDGEMENTS

Caroline Silva acknowledges CAPES-Proex (number 88887.288287-2018-00), for financial support. Moreover, the team ITAndroids would like to thank its sponsors: Altium, Intel, ITAEx, Mathworks, Metinjo, Micropress, Polimold, Rapid, Solidworks, ST Microelectronics, TFG, and Virtual Pyxis. Finally, the authors thank the support of the São Paulo Research Foundation – FAPESP (grant 2016/03647-3).

7. REFERENCES

Coelho, A.A.R. and Coelho, L.S., 2004. *Identificação de Sistemas Dinâmicos Lineraes*. Editora da UFSC, Santa Catarina, 1st edition.

Collins, S.H., Ruina, A., Tedrake, R. and Wisse, M., 2005. "Efficient bipedal robots based on passive-dynamic walkers". *Science*, Vol. 307, No. 5712, pp. 1082 – 1085.

Cotton, S., Murray, A.P. and Fraisse, P., 2009. "Estimation of the center of mass: From humanoid robots to human beings". *IEEE/ASME Transactions On Mechatronics*, Vol. 14, No. 6, pp. 707–712.

Ha, I., Tamura, Y. and Asama, H., 2013. "Development of open platform humanoid robot darwin-op". *Advanced Robotics*, Vol. 27, No. 3, pp. 223–232.

Kajita, S., Kanehiro, F., Kaneko, K., Yokoi, K. and Hirukawa, H., 2001. "The 3D Linear Inverted Pendulum Mode: A simple modeling for a biped walking pattern generation". In *Proc. Int. Conf. Intelligent Robots and Systems*. Maui, EUA, pp. 239 – 246.

Maximo, M.R.O.A., 2017. *Automatic walking step duration through model predictive control*. Ph.D. thesis, Instituto Tecnológico de Aeronáutica, São José dos Campos, Brasil.

Robotis OP2, 2019. "ROBOTIS-OP (a.k.a. DARWIN-OP) project". URL `https://sourceforge.net/projects/darwinop/files/Hardware/Mechanics/PhysicalInformation/`. Last accessed 25 July 2019.

Takenaka, T., Matsumoto, T. and Yoshiike, T., 2009. "Real Time Motion Generation and Control for Biped Robot -1st Report: Walking Gait Pattern Generation". In *Proc. Int. Conf. Intelligent Robots and Systems*. St. Louis, EUA, pp. 1084 – 1091.

van Zutven, P., 2014. *Control and Identification of Bipedal Humanoid Robots: Stability Analysis and Experiments*. Phd thesis, Eindhoven University of Technology.

Vukobratović, M. and Borovac, B., 2004. "Zero-Moment Point – Thirty Five Years of Its Life". *Int. J. Humanoid Robots*, Vol. 1, No. 1, pp. 157 – 173.

8. RESPONSIBILITY NOTICE

The authors are the only responsible for the printed material included in this paper.